THE JOURNAL OF BIOLOGICAL CHEMISTRY VOL. 283, NO. 36, pp. 24949–24961, September 5, 2008


# PAK Is Regulated by PI3K, PIX, CDC42, and PP2Cα and Mediates Focal Adhesion Turnover in the Hyperosmotic Stress-induced p38 Pathway*[S]

Received for publication, March 4, 2008, and in revised form, June 25, 2008 Published, JBC Papers in Press, June 27, 2008, DOI 10.1074/jbc.M801728200

**Perry M. Chan**[‡1], **Louis Lim**[‡§], **and Edward Manser**[‡]

*From the* [‡]*GSK-IMCB Group, Institute of Molecular and Cell Biology, Proteos Building, 61 Biopolis Drive, Singapore 138673 and the* [§]*Department of Molecular Neuroscience, Institute of Neurology, University College London, London WC1N 1PJ, United Kingdom*

**Fractionation of brain extracts and functional biochemical assays identified PP2Cα, a serine/threonine phosphatase, as the major biochemical activity inhibiting PAK1. PP2Cα dephosphorylated PAK1 and p38, both of which were activated upon hyperosmotic shock with the same kinetics. In comparison to growth factors, hyperosmolality was a more potent activator of PAK1. Therefore we characterize the PAK signaling pathway in the hyperosmotic shock response. Endogenous PAKs were recruited to the p38 kinase complex in a phosphorylation-dependent manner. Overexpression of a PAK inhibitory peptide or dominant negative Cdc42 revealed that p38 activation was dependent on PAK and Cdc42 activities. PAK mutants deficient in binding to Cdc42 or PAK-interacting exchange factor were not activated. Using a panel of kinase inhibitors, we identified PI3K acting upstream of PAK, which correlated with PAK repression by pTEN overexpression. RNA interference knockdown of PAK expression reduced stress-induced p38 activation and conversely, PP2Cα knockdown increased its activation. Hyperosmotic stress-induced PAK translocation away from focal adhesions to the perinuclear compartment and resulted in disassembly of focal adhesions, which are hallmarks of PAK activation. Inhibition of PAK by overexpression of PP2Cα or the kinase inhibitory domain prevented sorbitol-induced focal adhesion dissolution. Inhibition of MAPK pathways showed that MEK-ERK signaling but not p38 is required for full PAK activation and focal adhesion turnover. We conclude that 1) PAK plays a required role in hyperosmotic signaling through the PI3K/pTEN/Cdc42/PP2Cα/p38 pathway, and 2) PAK and PP2Cα modulate the effects of this pathway on focal adhesion dynamics.**

PAK,[2] the p21-activated kinase, is an effector kinase for the small Rho GTPases Cdc42 and Rac (1). PAKs mediate cytoskeletal rearrangements promoted by the activated GTPases such as loss of focal adhesions and actin stress fibers and the generation of filopodia (2, 3). PAK has also been implicated in other cellular events, including protection from apoptosis through phosphorylation of BAD (4, 5), mitosis through phosphorylation of RAF-1 (6, 7), and hormone signaling through estrogen receptor phosphorylation (8). The mitogen-activated protein kinase (MAPK) pathway is linked to PAK through Cdc42-mediated activation of p38, JNK (9), and ERK (10). The signaling pathways of extracellular stimuli leading to PAK and MAPK activation are not well characterized.

Changes in extracellular osmolality rapidly induce the activation of MAPKs (11); however, little is known of the regulators of the MAPK pathway. In *Saccharomyces cerevisiae*, stress response is mediated through specific osmosensing pathways, of which components include the MAPKs (12). The mammalian counterpart of these osmosensors has not been conclusively identified, although clustering of epidermal growth factor receptor has been proposed (13). PAK has been implicated in the stress response pathway through its activation upon hyperosmotic shock (14, 15).

The mechanism of PAK activation has been well studied. For Rho GTPase-dependent activation, the current model is based on the binding of the small G protein to the Cdc42/Rac interaction/binding (CRIB) region of PAK1. Because the CRIB region overlaps the kinase inhibitory domain (KID), this binding alleviates the autoinhibitory interactions between the KID and the catalytic domains (16, 17). Autophosphorylation of a serine residue in the KID and a threonine residue in the activation loop stabilizes the activated conformation of the kinase (18). A Rho GTPase-independent mechanism of kinase activation through GIT1 has also been described (19).

For the negative regulation of PAK1 by exogenous factors, far less is known. Studies from our group and others have identified protein serine/threonine phosphatases POPX1/2 (20) and PP2A (21, 22), and PAK-associated proteins hPIP1 (23) and merlin (24) as PAK inhibitors. Here, we identified PP2Cα as a major component of PAK1 inhibition *in vitro* and *in vivo*. PP2Cα has been shown to be involved in the down-regulation of the stress responsive p38 MAPK pathway (12, 25). In cells, hyperosmotic shock is a strong inducer of PAK activation, which results in morphological changes consistent with

* This work was supported by the GlaxoSmithKline-Singapore Research Fund (to E. M. and L. L.). The costs of publication of this article were defrayed in part by the payment of page charges. This article must therefore be hereby marked "*advertisement*" in accordance with 18 U.S.C. Section 1734 solely to indicate this fact.

[S] The on-line version of this article (available at http://www.jbc.org) contains supplemental Tables A–C and Figs. S1 and S2.

[1] To whom correspondence should be addressed. Tel.: 65-6586-9546; Fax: 65-6774-0742; E-mail: perryc@imcb.a-star.edu.sg.

[2] The abbreviations used are: PAK, p21-activated kinase; MAPK, mitogen-activated protein kinase; PI3K, phosphoinositide 3-kinase; MRCK, myotonic dystrophy kinase-related Cdc42-binding kinase; JNK, c-Jun $NH_2$-terminal kinase; ERK, extracellular signal-regulated kinase; KID, kinase inhibitory domain; RNAi, RNA interference; HA, hemagglutinin; GFP, green fluorescent protein; GST, glutathione *S*-transferase; siRNA, small interfering RNA; DMSO, dimethyl sulfoxide; SH, Src homology.

PAK activation. We showed that PAK activation by this stress required phosphoinositide 3-kinase (PI3K) activity, and PAK binding to Cdc42 and PIX. We also demonstrate through RNAi knockdown and KID or PP2Cα overexpression that PAK activity is essential for stress-induced p38. PP2Cα also protected cells from osmo-induced morphological changes arising from PAK activation. We conclude that multiple proteins regulate PAK in the hyperosmotic response pathway and PAK links cues from the extracellular environment to cytoskeletal dynamics.

## EXPERIMENTAL PROCEDURES

*Expression Constructs and Reagents*—Expression constructs of wild-type αPAK (rat PAK1) and its catalytically inactive and constitutively active variants, the PAK1 autoinhibitory fragment, the dominant active and negative variants of Cdc42, Rac and RhoA, and PIX were described previously (16, 26, 49). Wild-type pTEN and C124S mutant pTEN constructs were made from EST clones (Open Biosystems Inc.) and cloned into pXJ40 with HA tag. PP2Cα cDNA was kindly provided by Dr. Susanne Klumpp and subcloned into pXJ40 with a green fluorescent protein (GFP) tag for mammalian cell expression. Constructs of FLAG-tagged MAPKs p38, JNK, and ERK in pcDNA3 vector were gifts of Dr. Xinmin Cao. Recombinant PAK1 and PP2Cα were produced using bacterial expression vectors pGEX4T-1 (GE Healthcare) and pET16 (Novagen), respectively, and purified as glutathione *S*-transferase (GST) and hexahistidine fusion proteins as previously described (27). Anti-PP2Cα antibody was purchased from Upstate Biotechnology, anti-PP2A and anti-PP2B antibodies from Santa Cruz Biotechnology, and anti-tubulin and M2 anti-FLAG monoclonal antibodies (soluble and Sepharose-linked) from Sigma. The pan-PAK antibody, which does not discriminate between PAK isoforms, was purchased from Pharmingen, Inc. Phosphospecific antibodies against PAK, p38, JNK, and ERK were purchased from Cell Signaling Technology. Anti-PAK and anti-GIT1 antibodies were raised in rabbits and affinity purified. Anti-paxillin monoclonal antibody was purchased from ECM. Specific kinase and phosphatase inhibitors were from Sigma.

*Purification of PAK1 Phosphatase*—Rat brain lysate from 40 adult female rats was solubilized in homogenate buffer (20 mM HEPES pH 8.0, 100 mM NaCl, 1 mM $MgCl_2$, 0.1 mM EDTA, 0.2 mM phenylmethylsulfonyl fluoride, and 1 μg/ml each of leupeptin and aprotinin) with a Dounce homogenizer using 10 strokes. The lysate was pre-cleared by centrifugation at 100,000 × *g* for 30 min and the PAK1 phosphatase was followed in all subsequent steps by an *in vitro* activity assay described below. The activity was pelleted by a 30% ammonium sulfate cut after initial tests of adding varying concentrations of the salt to a fraction of the lysate. The pellet was solubilized in homogenate buffer and desalted by dialysis in the same buffer without NaCl. Phosphatase activity was retained in the dialyzed fraction from a 10-kDa molecular mass cutoff membrane (Pierce Biotechnology). At this point the total protein content was 0.6 g. All subsequent chromatographic separations were performed using the Pharmacia Fast Pressure Liquid Chromatography system. The dialyzed fraction was applied onto a DEAE-Sepharose column and a gradient of 0.01–1 M NaCl was used. Fractions (0.15–0.25 M NaCl) that contained phosphatase activity were pooled and dialyzed in mono-S buffer (10 mM Tris, pH 6.8, 10 mM NaCl, 1 mM $MgCl_2$, and 0.1 mM EDTA). This pool was applied onto a mono-S column and a gradient of 0.01–1 M NaCl was used for separation. Fractions 9–16 (corresponding to 0.2–0.36 M NaCl) contained the phosphatase activity and were pooled for immunodepletion of PP2Cα using sheep anti-PP2Cα antibody immobilized on protein A-Sepharose. Fractions before and after depletion were assayed for phosphatase activity.

*In Vitro Phosphatase Assays*—$^{32}P$ radiolabeled PAK1 was produced by autophosphorylation of recombinant GST-PAK in kinase buffer (50 mM HEPES, pH 7.4, 0.1 mM dithiothreitol, 10 mM $MgCl_2$, 0.5 mM ATP, and 1:100 (v/v) [$\gamma$-$^{32}P$]ATP) for 1 h at 30 °C. The protein was desalted through a NAP-5 column (GE Healthcare) and used as the substrate for phosphatase assays. Rat brain lysate fractions and recombinant PP2Cα were tested for activity by monitoring the loss of radiolabel from GST-PAK1 in a phosphatase reaction for 10 min at room temperature, using divalent cation-dependent phosphatase buffer (50 mM Tris, pH 7.4, 100 mM NaCl, 0.1 mM dithiothreitol, 10 mM $MgCl_2$, or 1 mM $MnCl_2$). The phosphatases PP1 and PP2A were purchased from Upstate Biotechnology. For comparison of different substrates, recombinant purified GST fusion proteins of PAK1 and -2, α and β myotonic dystrophy kinase-related Cdc42-binding kinase (MRCK), and protein kinase Cα were radiolabeled to maximal levels by kinase reaction for 3 h at 30 °C. The labeled proteins were then desalted through NAP-5 columns equilibrated with phosphatase buffer. Rates of dephosphorylation were calculated from densitometric analyses of autoradiograms and Western blots using ImageJ (National Institutes of Health, Bethesda, MD).

*Transfection of Mammalian Cells and Hyperosmolarity Response Assays*—COS7 and HeLa cells were transfected with the relevant constructs using Lipofectamine transfection reagent (Invitrogen). Cells were serum-starved for 4 h and the hyperosmolarity stress response was induced by adding sorbitol to 0.8 M for 30 min. For the kinase inhibition assay, drugs were added to culture medium 2 h before sorbitol shock. The carrier dimethyl sulfoxide was added as the negative control. The concentrations of drugs used are as follows: SB203580, 20 μM; SP600125, 30 μM; PD98059, 30 μM; LY294002, 20 μM; H89, 20 μM; wortmannin, 560 nM; genistein, 50 μM; SB216763, 20 μM; tyrphostin AG, 1 μM. For RNAi analyses, N1E-115 cells were transfected with 0.4 μM siRNAs using Lipofectamine 2000. At 48 h post-transfection, cells were treated with sorbitol and harvested for analysis.

*Immunoprecipitation and Blotting*—Following osmotic stress, cells were washed once in cold phosphate-buffered saline, pH 7.4, and harvested in lysis buffer (20 mM HEPES pH 7.4, 150 mM NaCl, 0.1 mM dithiothreitol, 1 mM EDTA, 1 mM EGTA, 1 mM sodium vanadate, 0.5 mM sodium fluoride, 10 nM okadaic acid, 0.2 mM phenylmethylsulfonyl fluoride, and 1 μg/ml each of leupeptin and aprotinin). Cell lysates were precleared by centrifugation and the relevant antibodies were added to the supernatant. The immunoprecipitates were washed 3 times with lysis buffer and eluted by boiling in SDS sample buffer for 2 min. Proteins were separated by SDS-PAGE and transferred onto polyvinylidene difluoride membranes

(Millipore). Membranes were blocked with 5% nonfat dry milk in phosphate-buffered saline containing 0.2% Tween 20 and probed with primary and secondary antibodies in the same buffer. For phospho-MAPK or phospho-PAK blots, 5% bovine serum albumin in Tris-buffered saline containing 0.5% Tween 20 was used for blocking and probing buffers.

*Cell Staining*—HeLa cells were treated with 0.8 M sorbitol for varying time points and fixed with 3% paraformaldehyde/phosphate-buffered saline. Endogenous PAK was detected using purified polyclonal anti-PAK antibody. Focal adhesions were probed using monoclonal anti-paxillin antibody. Anti-mouse and anti-rabbit secondary antibodies conjugated with Alexa 488 or Alexa 546 were used for visualization. Images were taken using ×40 oil-immersion objectives (Zeiss Axioplan) and analyzed using the MetaMorph software (Universal Imaging Corporation). For confocal analyses of microinjected fixed cells, images were taken also using 40× oil-immersion objectives mounted on a Zeiss LSM510 Meta system.

*Design of siRNAs Directed toward PAK and PP2Cα*—RNAi experiments were performed on N1E-115 cells as endogenous PAK and PP2Cα proteins are detectable in this cell line. Oligonucleotides for PCR were designed to amplify the 9–1012 base region of the mouse PAK gene, and the 12–995 base region of mouse PP2Cα. Gene fragments were PCR amplified using total cDNA from N1E-115 cells. For control, the 41–677 region of GFP was PCR amplified using miniprep DNA containing the GFP insert. The T7 promoter was appended to both 5′ and 3′ sequences. RNA corresponding to the gene regions was made using the *in vitro* T7 transcription kit (Ambion), and processed to ~25-mers using the ShortCut RNAi kit (New England Biolabs).

## RESULTS

*PP2Cα Is a Major PAK1 Inhibitory Component in Brain Extract*—The PAK family of kinases is regulated through multiple mechanisms, such as small GTPase binding, autophosphorylation, membrane targeting, and autoinhibition (3). We noted that endogenous PAK1 purified from brain extract was largely inactive (1), whereas recombinant PAK1 from *Escherichia coli* was highly activated (28). This led us to surmise that brain-specific factors maintain PAKs largely in a repressed state. Using recombinant PAK1, we detected a highly stable component of brain lysate that reversed kinase autophosphorylation (Fig. 1*A*). Kinase activity toward exogenous substrates such as myelin basic protein was also inhibited (data not shown). Using active $^{32}$P-radiolabeled PAK as a substrate, we determined that this component was a serine/threonine phosphatase that efficiently dephosphorylated PAK1. This phosphatase appeared to belong to the PPM family (29), as it was largely insensitive to okadaic acid inhibition and required divalent cations for activity (Fig. 1*B*). Partial purification and immunodepletion of brain lysate (supplemental Fig. S1) identified PP2Cα as the major active component that dephosphorylated PAK1 (Fig. 1*C*). Indeed, the PP2Cα-depleted fraction that contained other phosphatases such as POPX1/2, PP2A, and PP2B was selectively compromised in its capacity to dephosphorylate PAK1. Although other PAK1-directed phosphatases cannot be ruled out in this *in vitro* assay, these results suggest that PP2Cα is the major inhibitor of PAK1 in the brain lysate.

Recombinant PP2Cα behaved similarly to the major phosphatase activity in brain lysate, in terms of okadaic acid and microcystin sensitivity, divalent cation dependence, and heat stability (68 °C for 10 min; data not shown). Purified PP2Cα protein efficiently dephosphorylated PAK1 *in vitro* (Fig. 1, *D* and *E*). We previously assessed the time course of phospho-PAK1 dephosphorylation assessed using specific antibodies against either Ser(P)$^{198/203}$ or Thr(P)$^{422}$ sites in the PAK1 activation loop. Both sites were dephosphorylated with the same kinetics; the anti-Ser(P)$^{198}$ antibody was subsequently used as it exhibited lower background staining. Direct comparison of PP2Cα with purified PP1 and PP2A lead us to conclude that at the same molar ratio PP2Cα was the most efficient in dephosphorylating PAK1 (Fig. 1*D*). In this case we monitored two autophosphorylation sites in the Pak1 N-terminal regulatory region (Ser$^{57}$ and Ser$^{198/203}$) using phosphospecific antibodies: both sites showed the same kinetics of inactivation. Furthermore, PP2Cα was more active toward PAK than a number of other autophosphorylated kinases (Fig. 1*E*). For example, PP2Cα displayed more complete dephosphorylation of PAK1 and PAK2 than α and β isoforms of the MRCK or protein kinase Cα. Overexpression of PP2Cα did not reveal any changes in focal adhesion (Fig. 6*A*) or filamentous actin dynamics in unstimulated cells (data not shown).

*PAK Is Activated and Targets to p38 in Hyperosmotic Signaling*—To verify that PAK and p38 are involved simultaneously in this pathway, we examined the association of PAK with MAPKs and the kinetics of activation. First, overexpressed PAK1 was most potently activated by sorbitol relative to serum, epidermal growth factor, or platelet-derived growth factor (Fig. 2*A*). The kinetics of PAK1 activation closely paralleled that of p38 (Fig. 2*B*), suggesting tight coordination of the two kinases in this stress response. Cells treated with increasing concentrations of sorbitol display proportionate increases in levels of phosphorylated p38, c-Jun N-terminal kinase (JNK), and extracellular signal-regulated kinase (ERK) (Fig. 2*C*). Immunoprecipitation of MAPK complexes revealed that endogenous PAKs associated with activated p38 but not with activated JNK or ERK. The formation of the phosphorylated PAK-p38 complex was readily detected in the p38 immunocomplex at 0.8 M sorbitol. The presence of multiple type I PAK isoforms in the p38 complex suggests functional redundancy. This is supported by the increase in levels of endogenous osmo-induced phospho-p38 when transfected with type I PAK isoforms (Fig. 2*D*). The level of endogenous phospho-p38 is dependent on transfection efficiency.

Upon activation, the PAK KID dissociates from the catalytic domain leading to autophosphorylation at multiple sites (for example Ser$^{57}$, Ser$^{198}$, Ser$^{203}$, and Thr$^{422}$). A constitutively active PAK1$^{L107F}$ with mutated KID displayed better binding to the p38 complex *versus* wild-type or an open conformation but kinase-inactive PAK1$^{L107F/T422A}$ version (Fig. 2*E*).

*PAK1 and p38 Are Regulated by PP2Cα in Vivo*—Both PAK1 and PP2Cα have been implicated in regulation of stress response signaling (25, 30–32). We therefore went on to investigate how they may interact in this pathway. Overexpressed

PP2Cα inhibited stress activation of both PAK1 and endogenous p38 to basal levels (Fig. 3*A*, supplemental Fig. S2*B*). The level of phosphatase in COS7 and HeLa cell lines was much lower than in brain by Western blotting (data not shown). Regarding PP2Cα specificity toward type I PAKs, the phosphatase antagonized p38 phosphorylation irrespective of the PAK

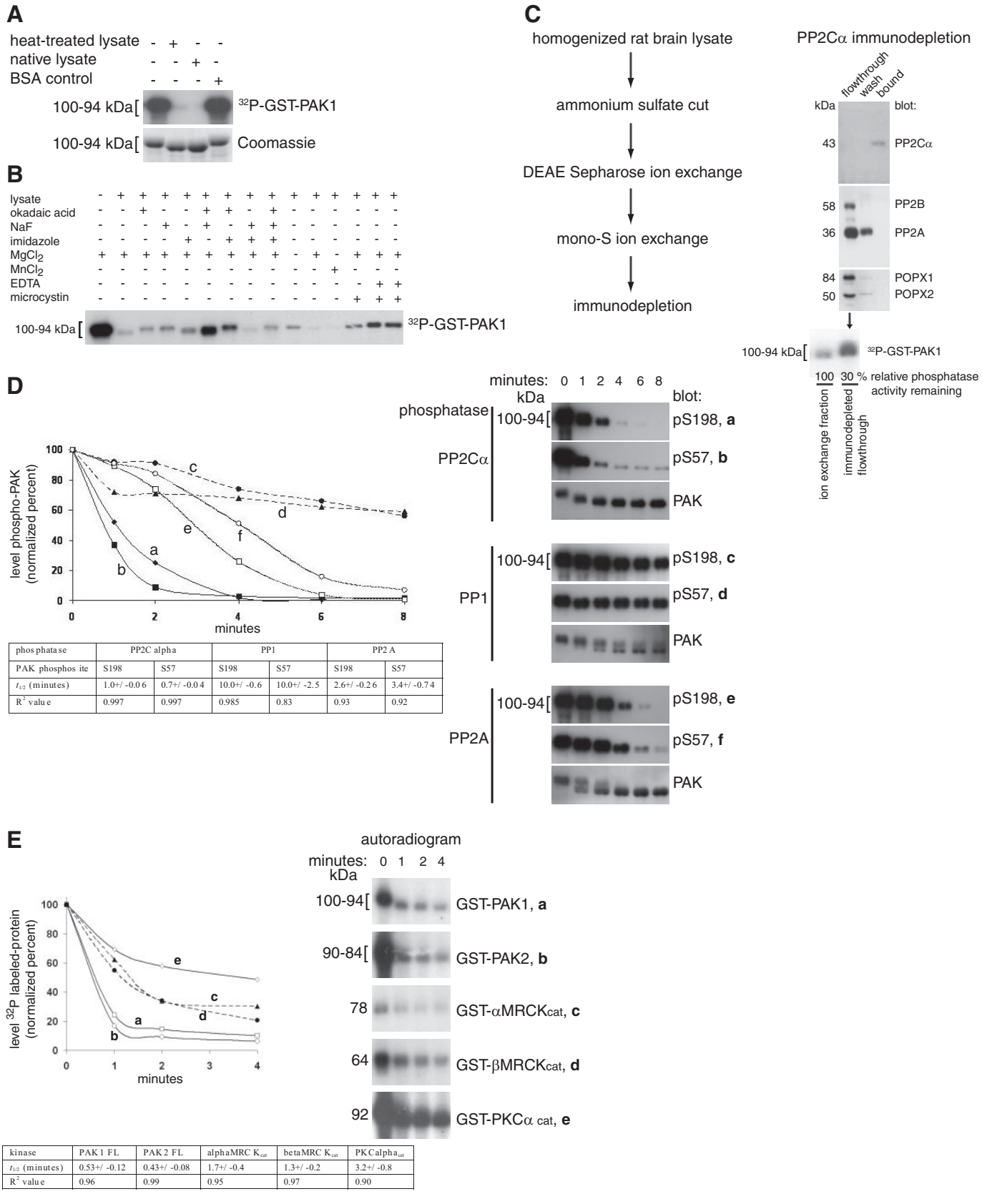


| phosphatase | PP2C alpha | | PP1 | | PP2 A | |
|---|---|---|---|---|---|---|
| PAK phosphosite | S198 | S57 | S198 | S57 | S198 | S57 |
| $t_{1/2}$ (minutes) | 1.0+/ -0.06 | 0.7+/ -0.04 | 10.0+/ -0.6 | 10.0+/ -2.5 | 2.6+/ -0.26 | 3.4+/ -0.74 |
| $R^2$ value | 0.997 | 0.997 | 0.985 | 0.83 | 0.93 | 0.92 |

| kinase | PAK1 FL | PAK2 FL | alphaMRC $K_{cat}$ | betaMRC $K_{cat}$ | PKCalpha$_{cat}$ |
|---|---|---|---|---|---|
| $t_{1/2}$ (minutes) | 0.53+/ -0.12 | 0.43+/ -0.08 | 1.7+/ -0.4 | 1.3+/ -0.2 | 3.2+/ -0.8 |
| $R^2$ value | 0.96 | 0.99 | 0.95 | 0.97 | 0.90 |

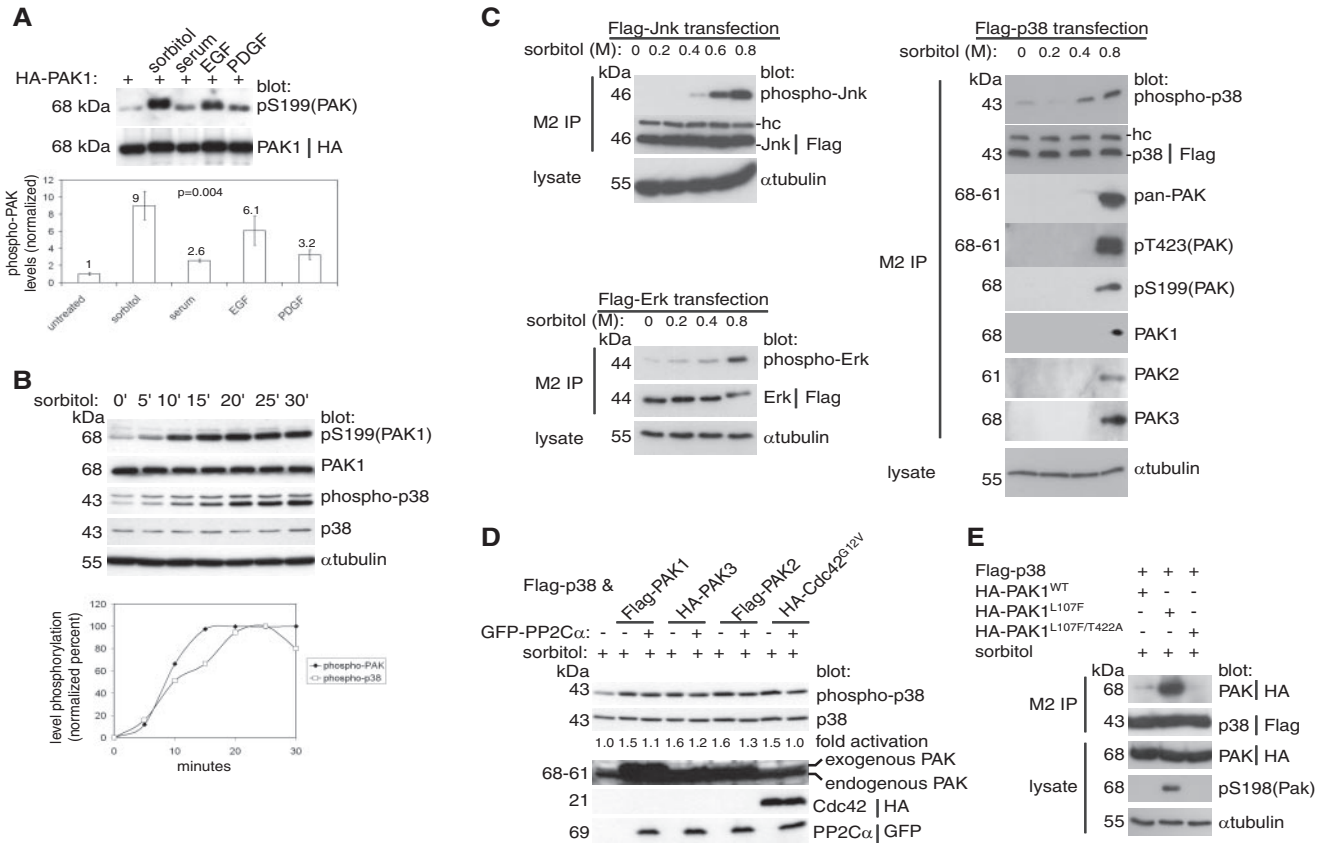


FIGURE 2. **Characterization of PAK1 and p38 in hyperosmotic shock.** *A*, sorbitol is a potent activator of PAK1. COS7 cells were transfected with HA-PAK1, and treated with or without sorbitol for 30 min, or serum (10%), epidermal growth factor, or platelet-derived growth factor (100 ng/ml) for 10 min. Levels of phospho-PAK1 were quantitated by densitometric analysis of Western blots. Phospho-PAK1 in untreated cells was standardized at the value of 1 and other treatment conditions were normalized to that value. Mean values of two independent assays are labeled *above the bars*. Statistical analysis using one-way analysis of variance yielded the *p* value of 0.004. *B*, kinetics of PAK1 and p38 activation align closely under high osmolarity. In COS7 cells overexpressing HA-PAK1 and FLAG-p38, treatment with 0.8 M sorbitol resulted in similar kinetics for PAK1 and p38 activation, as assessed by phospho-PAK1 and phospho-p38 Western blotting. *C*, PAK is activated and recruited to the p38 complex under high osmolarity. In HeLa cells transfected with FLAG-tagged p38, endogenous PAKs was activated (as detected by PAK phospho-specific antibodies; residue numbers according to human PAK) and recruited to the phospho-p38 complex at high concentrations of sorbitol. Activation of JNK, p38, and ERK was proportional to increasing concentrations of sorbitol, as probed by phospho-specific MAPK antibodies. PAK did not co-precipitate with phospho-JNK or phospho-ERK under the conditions used (data not shown). *M2 IP* and *hc* represent M2 anti-FLAG immunoprecipitation complexes and IgG heavy chain, respectively. *D*, overexpression of group I PAKs can augment hyperosmotic-induced p38 phosphorylation. Cells were transfected with PAK1, -2, -3, or dominant active Cdc42, alone or together with PP2Cα, and treated with sorbitol. Endogenous phospho-p38 was elevated by overexpression of PAKs or $Cdc42^{12V}$, and decreased by PP2Cα. Levels of phospho-p38 was quantitated by densitometry and normalized to the p38 response in untransfected cells. *E*, constitutively active PAK1 co-precipitated with the p38 complex following hyperosmotic shock. COS7 cells co-transfected with FLAG-p38 and wild-type, L107F (constitutively active), or L107F/T422A (open conformation, non-activable) versions of PAK1 were treated with 0.8 M sorbitol for 30 min. The constitutively active PAK1 displayed higher affinity than the wild-type kinase for the p38 complex.

isoform overexpressed (Fig. 2*D*). To establish that endogenous PAK and PP2Cα regulate p38 *in vivo*, we targeted the two genes in N1E-115 cells by RNA interference using random dicer-generated pools of short double-stranded RNA corresponding to the N termini of the kinase and phosphatase (Fig. 3*B*). PAK1 is the dominant isoform in neuronal cells. RNAi knockdown of

FIGURE 1. **Identification and characterization of PP2Cα as the major phosphatase of PAK1 in brain lysate.** *A*, detection of PAK1 inhibitory activity in rat brain lysate. Recombinant GST-PAK1 (0.24 mg/ml) was used in a kinase assay with native or heat-treated (68 °C for 10 min) lysates, or an equal amount of bovine serum albumin (*BSA*) for control (0.1 mg/ml). The kinase reactions were incubated at 30 °C for 10 min in the presence of [γ-$^{32}$P]ATP and terminated by adding SDS-sample buffer and boiling for 2 min. Following SDS-PAGE, incorporated $^{32}$P-labeled phosphate was visualized by autoradiography (*top panel*); phosphorylation of PAK1 resulted in its decreased mobility (*bottom panel*). *B*, characterization of phosphatases in brain lysate acting on PAK1. PAK phosphatase activity in lysate was assayed in the presence of protein serine/threonine phosphatase inhibitors okadaic acid (0.1 μM), sodium fluoride (2 mM), or imidazole (1 mM). Divalent cation dependence of the phosphatase was tested using $MgCl_2$ (10 mM), $MnCl_2$ (1 mM), and the cation chelator EDTA (50 mM). Okadaic acid and microcystin showed inhibitory activity only at concentrations higher than 2 μM and 200 nM, respectively. *C*, scheme of biochemical fractionation and PP2Cα immunodepletion of brain lysate. Fractions separated by mono-S chromatography that contained phosphatase activity on PAK1 (supplemental Fig. 1) were pooled and passed through a column containing anti-PP2Cα antibody immobilized on protein A-Sepharose. The depleted fraction (flow-through) and pre-depleted lysate in equal amounts were compared for PAK1 phosphatase activity. Western blotting of crude brain extract with the anti-PP2Cα antibody showed a single band at 42 kDa (data not shown). The flow-through, wash, and bound fractions were analyzed for the presence of protein serine/threonine phosphatases PP2A, PP2B, POPX1, and POPX2 by Western blotting. *D*, comparison of PP2Cα, PP1, and PP2A phosphatase activities on pre-activated PAK1. The three phosphatases were used in equal molar concentrations (0.9 μM) and dephosphorylation of PAK1 was followed by Western blotting for Ser(P)$^{57}$ and Ser(P)$^{198}$, two known PAK phosphosites. Dephosphorylation of PAK1 was most efficiently performed by PP2Cα (*curves a* and *b*), followed by PP2A (*e* and *f*), and last, PP1 (*c* and *d*). The $t_{1/2}$ (reaction time required to dephosphorylate 50% of phospho-protein) and $R^2$ values were obtained by statistical curve fitting of densitometric values. *E*, comparison of PAK isoforms and other protein serine/threonine kinases as substrates for PP2Cα. The recombinant protein kinases were purified to >95%, pre-phosphorylated in the presence of [γ-$^{32}$P]ATP and used at the same concentration of 24 μg/ml. PP2Cα was added to a concentration of 0.05 μg/ml to initiate the reaction. PP2Cα most efficiently dephosphorylated full-length PAK1 and PAK2, followed by αMRCK and βMRCK catalytic domains and finally PKCα catalytic domain.

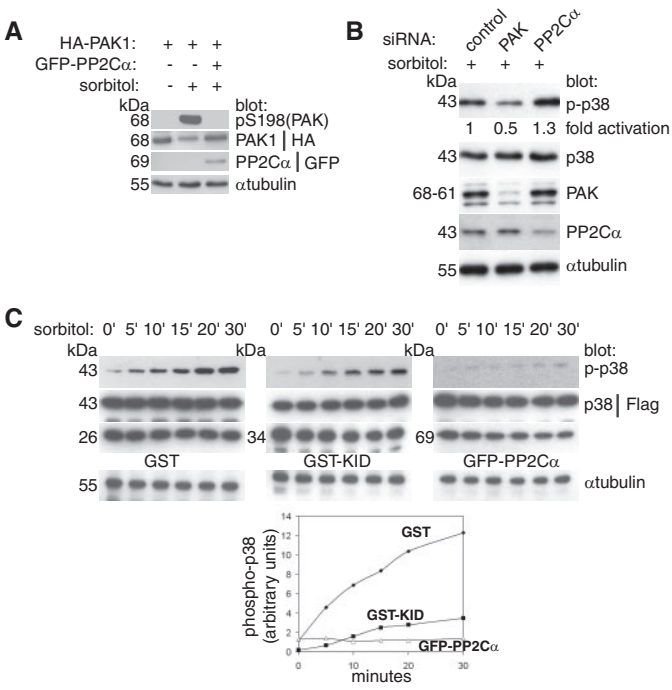


FIGURE 3. **Characterization of PAK1 and p38 regulation by PP2Cα phosphatase in the hyperosmotic response.** *A*, overexpression of PP2Cα phosphatase down-regulated both PAK1 and endogenous p38. COS7 cells transfected with FLAG-tagged wild-type PAK1, with or without PP2Cα, were treated with sorbitol for 30 min. Levels of both phospho-PAK1 and endogenous phospho-p38 were decreased in the presence of elevated phosphatase. *B*, effects of RNAi knockdown of PAK and PP2Cα on p38 phosphorylation. N1E-115 cells transfected with siRNA targeting PAK (resulting in 75% knockdown) displayed reduced stress activation of p38 to ~50% of normal, and cells transfected with siRNA targeting PP2Cα (50% knockdown) up-regulated p38 to 130% above normal. The control siRNA directed against GFP had no effect. N1E-115 cells were used because endogenous levels of PAK and PP2Cα are easily detectable. *C*, the inhibition of PAK *versus* PP2Cα overexpression was compared for the efficacy and duration of p38 inhibition. COS7 cells were transfected with FLAG-p38 together with GST, GST-KID (PAK1 kinase inhibitory domain peptide; residues 83–149), or GFP-PP2Cα for 24 h before sorbitol treatment. Overexpression of the phosphatase had a stronger effect on reducing p38 phosphorylation than inhibition of PAK.

PAK (~75% knockdown) reduced sorbitol-induced p38 activation to 50% of normal. Conversely, RNAi knockdown of PP2Cα (~50% knockdown) enhanced p38 activation to levels 130% above normal. The control RNAi targeting GFP generated by the same method had no effect on protein expression or p38 phosphorylation. We compared the effects of KID or PP2Cα overexpression on p38 activation kinetics (Fig. 3*C*). PAK inhibition mediated by KID resulted in delayed and decreased phosphorylation of p38, whereas PP2Cα resulted in a more complete inhibition of p38. The GST control had no effect. This additive inhibition of p38 by PP2Cα relative to KID suggests that the phosphatase acts not only on PAK but also other components of the pathway.

*PAK Activation Is Mediated by PI3K/Cdc42 Activities and PIX Binding*—PAK exists as part of a multimeric complex containing PIX and GIT, which target the kinase to subcellular compartments and are involved in Rho GTPase-mediated activation of PAK (1, 49). We investigated the role of Rho GTPases and PAK binding partners in osmo-induced PAK activation. Overexpression of dominant negative p21s showed that Cdc42 was closely coupled to PAK in this pathway (Fig. 4*A*). Direct inhibition of PAK through KID overexpression was comparable with dominant negative Cdc42 specifically on p38 phosphorylation but not on JNK (Fig. 4*B*). We assessed the role of PIX, Cdc42, and NCK binding on PAK activation by using mutants that are specifically deficient in binding these upstream regulators: S76P abolishes Cdc42 binding; P191G/R192A abolishes PIX binding; Δ22 N terminus (Δ22N.T.) abolishes NCK binding. The S198A/S203A (phosphorylation sites in the KID) and T422A (activation loop) mutants were used as negative controls. Binding to Cdc42 and PIX but not NCK are required for PAK activation in this pathway (Fig. 4*C*). The Cdc42 and PIX binding-deficient PAK mutants consistently migrate slower than the wild-type kinase, possibly due to a more opened conformation despite not being activated. To probe other signaling proteins involved in this pathway, we used inhibitors to assess the kinases upstream of PAK and p38. LY29004 and wortmannin, inhibitors of PI3K, potently inhibited both PAK and p38 activation (Fig. 4*D*). Overexpression of $pTEN^{WT}$ but not the $pTEN^{C124S}$ inactive mutant significantly reduced PAK activation (Fig. 4*E*), suggesting the generation of phosphorylated phosphatidylinositol(s) is required for efficient PAK1 activation in this pathway. Interestingly PD98059, an inhibitor of MEK, also inhibited PAK but not p38, suggesting the presence of a feedback loop between PAK and MEK-ERK. These results suggest PI3K activity is required for PAK hyperosmotic activation.

*PAK Activity Is Involved in Hyperosmotic Stress-induced Changes in Focal Adhesions*—As sorbitol was an activator of PAK (Fig. 2*A*), we examined its effects on cellular focal adhesion dynamics. Our group and others have shown PAK activity results in robust disassembly of focal adhesions (36), which can be quantified because of their distinct localization and structure. In the lamella region of cells, immunofluorescence signals at adhesion complexes using a sensitive pan-PAK antibody yielded endogenous PAK signals that overlapped 55 ± 3% of pixels positive for paxillin in adhesions; the localization of PAK occurs at the distal end of adhesion complexes (Fig. 5*A*, supplemental Table A). In HeLa cells, this signal derives primarily from the PAK2 isoform. Sorbitol treatment resulted in significant loss of adhesion-localized PAK to only 26% overlap; visual inspection indicates an even more significant loss of PAK staining at adhesions. Loss of focal adhesions (as assessed by paxillin signal, see legends for details) was concomitant with PAK activation, with the average focal adhesion-localized paxillin signal at 43 ± 7% in sorbitol-treated *versus* control cells. We then examined endogenous GIT1, a PAK-binding partner responsible for bringing the kinase to adhesion complexes (36). In untreated cells, anti-GIT1 signals were colocalized 73 ± 2% of pixels in paxillin containing adhesions: this ratio was essentially unchanged at 75 ± 2% of paxillin following osmotic stress (Fig. 5*B*, supplemental Table A), indicating that the focal adhesion-localized GIT1-paxillin interaction was unaffected by osmotic shock. These results suggest that osmotic shock activates PAK and causes its translocation away from the multimeric complex containing GIT1 (and PIX) at focal adhesions. Antibodies against PIX were less sensitive than GIT1 for immunofluorescence.

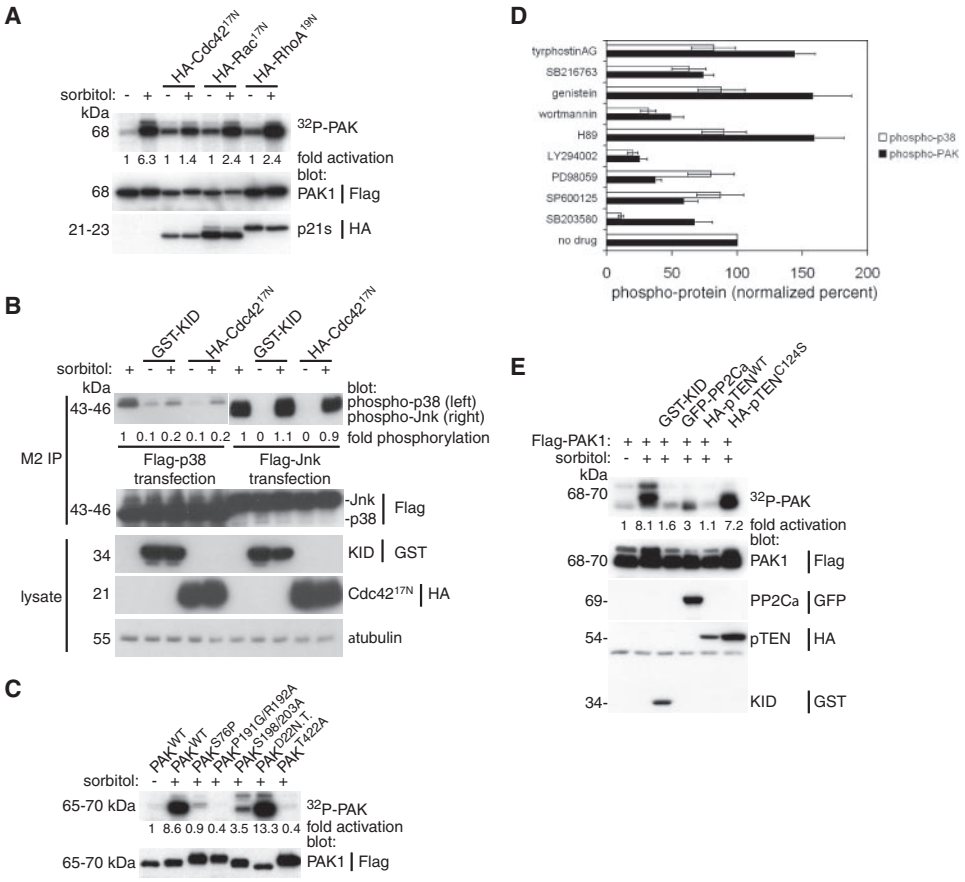


FIGURE 4. **Role of Rho GTPases and binding requirements for PAK1 and p38 signaling.** *A*, the role of Cdc42, Rac, and RhoA on osmoinduced PAK1 activation was examined. COS7 cells were transfected with dominant-negative versions of the Rho GTPases and FLAG-PAK1. Levels of PAK1 activity were assessed for cells with or without sorbitol treatment by immunoprecipitating PAK1 and assessing autophosphorylation of the kinase in the presence of [$^{32}$P]ATP for 10 min at 30 °C. This showed that interfering with Cdc42 strongly reduced sorbitol activation of PAK1. The basal levels of PAK1 in untreated cells for each Rho GTPase were standardized to 1. PAK fold activation was measured by densitometric analyses of autoradiograms. *B*, overexpression of GST-KID peptide or dominant-negative Cdc42 inhibited activation of p38 but not of JNK. COS7 cells were transfected with FLAG-p38 or FLAG-JNK alone, or cotransfected with GST-KID or HA-Cdc42$^{17N}$ before sorbitol treatment. *C*, role of PAK1-interacting partners in kinase activation. PAK mutants defective in binding specific proteins were used: *S76P*, defective in Cdc42 binding; *P191G/R192A*, defective in PIX binding; *Δ22N.T.* ($NH_2$ terminus), defective in NCK binding; *S198/203A* and *T422A*, negative controls as non-activable kinases. FLAG-PAK wild-type and mutants were transfected and analyzed for osmo-induced activity as in *A*. PAK mutants defective in Cdc42 and PIX binding consistently showed slower mobility than the wild-type kinase, despite not being activated in these assays. *D*, PI3K/Cdc42/PAK signaling pathway leads to stress-induced p38 phosphorylation. COS7 cells were transfected with FLAG-PAK1 and FLAG-p38 and treated with the indicated drugs 2 h prior to osmotic shock. DMSO (no drug) was used as the control and normalized to 100% of phosphorylated kinase. Phosphorylated PAK and p38 were assessed by Western blotting and quantitated by densitometry. The PI3K inhibitors LY294002 and wortmannin significantly inhibited both PAK and p38 phosphorylation. Statistical analyses using one-way analysis of variance yielded a *p* value of 0.002 for phospho-PAK assays and a *p* value of 0.012 for phospho-p38 assays. *E*, COS7 cells were transfected with FLAG-PAK1 alone or cotransfected with GST-KID, GFP-PP2Cα, HA-pTEN$^{WT}$, or HA-pTEN$^{C124S}$ (inactive phosphatase) and subjected to osmotic shock. Overexpression of pTEN$^{WT}$ but not HA-pTEN$^{C124S}$ suppressed PAK1 activation to similar levels as KID and PP2Cα.

plemental Fig. S2). We also investigated whether the phosphatase localized with PAK or focal adhesion structures during the osmotic response. Antibody against PP2Cα was not suitable for immunostaining (data not shown). Plasmid microinjection of GFP-PP2Cα in HeLa cells allowed assessment of GFP localization only 1 h post-injection at low levels. Confocal analyses of untreated and sorbitol-treated cells showed that GFP-PP2Cα translocated from the cytosol to membrane regions that overlap with focal adhesions (supplemental Fig. S3*B*). Overexpression of PP2Cα also resulted in stronger PAK staining and kinase retention at focal adhesions in sorbitol-treated cells (supplemental Fig. S3*A*).

*MEK/ERK Pathway Is Involved in Hyperosmotic Stress-induced Changes in Focal Adhesions*—As the MAP kinases p38, JNK, and ERK were all activated by osmotic stress (Fig. 2*C*), we examined the contribution of MAPK signaling to focal adhesion loss using kinase inhibitors (Fig. 7). Inhibition of p38 using SB203580 (61% decrease) and inhibition of JNK using SP600125 (58% decrease) were essentially unchanged from DMSO controls (71% decrease). However, inhibition of MEK using PD98059 (20% decrease) significantly protected focal adhesions from disassembly (Fig. 7*D*). This correlates with the effects of PD98059 on PAK activity, although this class of inhibitor does not effect PAK kinases (57). Statistical calculations are described in supplementary Table C. We went on to test if PAK is involved directly in this stress activation of the MEK-ERK pathway. Inhibition of PAK through overexpression of KID had no effect on sorbitol-induced ERK activation (Fig. 7*E*), whereas ERK phosphorylation was abolished in the presence of PD98059, suggesting that PAK is not upstream of MEK-ERK in this stress response pathway but rather MEK-ERK is involved in the kinase activation.

Inhibition of PAK activation via overexpressed PP2Cα or KID protected focal adhesions from osmotic-induced disassembly (Fig. 6, *A* and *B*). For PP2Cα-transfected cells, average focal adhesion size decreased 29 ± 2% in sorbitol-treated cells, compared with a loss of 66 ± 4% in nontransfected cells in the same fields with sorbitol treatment. For KID-expressing cells, paxillin levels decreased 11 ± 1% after sorbitol shock compared with a decrease of 62 ± 21% in untransfected cells; thus PAK in these cells is indeed directly implicated in turnover of focal adhesions. Immunostaining of phospho-PAK or phospho-p38 in cells expressing PP2Cα confirmed that the phosphatase reduced sorbitol-induced PAK and p38 phosphorylation (sup-

## DISCUSSION

*Phosphatase-mediated Down-regulation of PAK*—PAK activity has been associated with cellular events such as cytoskeletal rearrangements, neurite outgrowth, proliferation, and apoptosis (2, 3, 33). These events involve cycles of activation and inac-

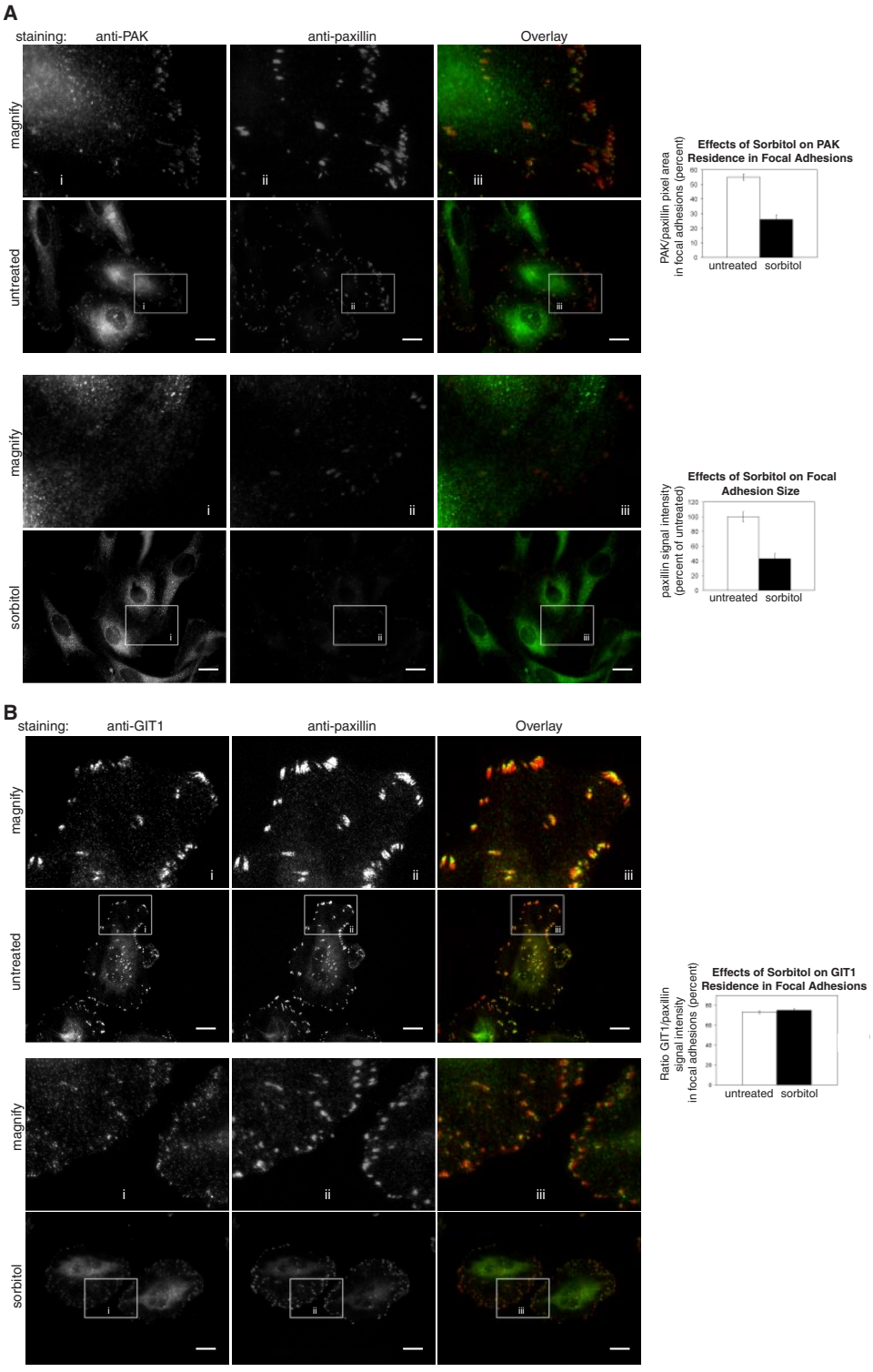


FIGURE 5. **Analyses of PAK, GIT1, and paxillin loss during osmo-induced focal adhesion disassembly.** *A*, HeLa cells were examined for effects of sorbitol treatment on adhesion-associated endogenous PAK, GIT1, and paxillin, which defines focal adhesion size. Immuno-staining conditions and data collection were identical between pairs (sorbitol treated *versus* untreated). Cells were plated at low density to allow for efficient spreading, and the fields of analysis were arbitrarily chosen. Regions in the cell lamella zone (away from cell body) were selected and the paxillin signals were used to define the adhesion volume using identical threshold parameters (set by the local cytosolic signal). For each paxillin-positive pixel we scored if the pixel space was also PAK-positive; colocalization percentage represents PAK-positive signal area/paxillin-positive signal area. For the sorbitol-treated cells, PAK staining after threshold assessment gives punctate random signals that contribute to "PAK-positive" pixel area, although this is likely random colocalization. For focal adhesion "size" analysis, thresholds were again set to isolate focal adhesions and paxillin-integrated fluorescence levels were quantitated within each area. This yields total paxillin signal at focal adhesions. This is repeated for each randomly selected lamella region; the mean paxillin signal per adhesion is the sum of all the integrated intensity values divided by the number of focal adhesions. *Error bars* on the graphs represent S.E. values. Statistics are further detailed in supplemental Table A. Sorbitol caused PAK loss from focal adhesions (over 2-fold relative to untreated) and the loss of focal adhesion integrity as measured by paxillin staining (over 2-fold relative to untreated). Regions within the images (*rectangles* with corresponding labels *i*, *ii*, and *iii*) were magnified for visualization. *B*, effects of sorbitol on translocation of endogenous GIT1 was examined. In contrast to PAK, GIT1 remained stably associated with focal adhesions after osmotic shock. *Bars* on images are equivalent to 20 $\mu$m; two independent fields were analyzed for quantitation.

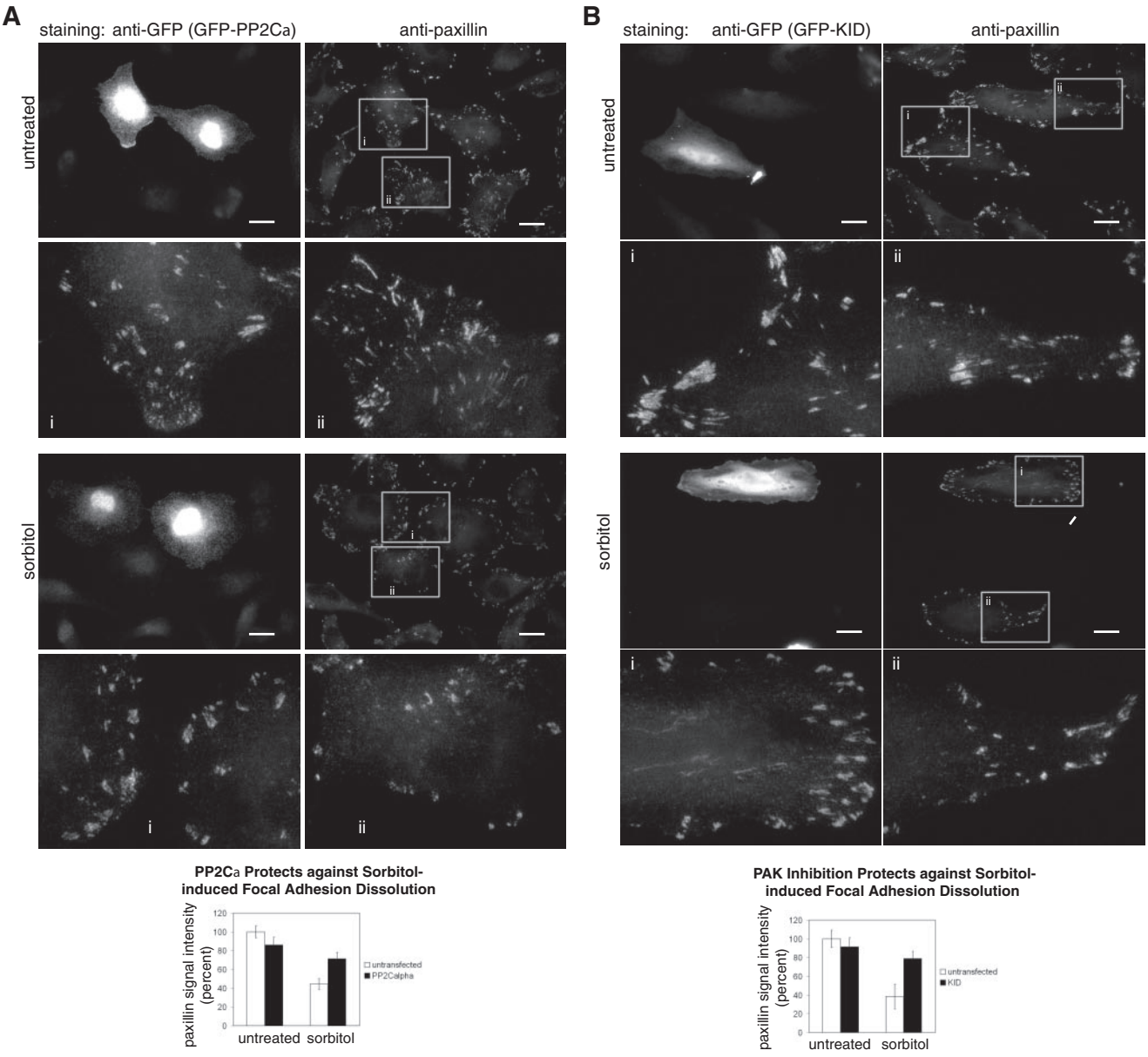


FIGURE 6. **Effects of PAK inhibition on osmo-induced focal adhesion disassembly.** *A*, HeLa cells transfected with GFP-PP2C$\alpha$ (stained with anti-GFP antibody) showed protection of focal adhesion integrity compared with untransfected cells after sorbitol treatment. Focal adhesions of untransfected, untreated cells were standardized to 100% and used for normalization. After sorbitol treatment, the focal adhesions of GFP-PP2C$\alpha$ expressing cells were compared with those of non-expressing cells. In the absence of sorbitol treatment, there was no significant difference between transfected and untransfected cells. Statistics are documented in supplemental Table B. *B*, HeLa cells transfected with GFP-KID (stained with anti-GFP antibody) similarly showed protection from focal adhesion dissolution compared with untransfected cells after sorbitol treatment. No significant difference was observed between transfected and untransfected cells without sorbitol. *Bars* on images are equivalent to 20 $\mu$m; two independent fields were analyzed for quantitation.

tivation and therefore conceptually would require diverse mechanisms to regulate this family of kinases. Indeed, the kinase activation of group I PAKs is governed at multiple levels, the normal autoinhibition in *trans* by its KID is alleviated by binding Rho GTPase partners (and lipids) and by potential upstream activating kinases such as PDK1 (34, 35). We show here that elevated levels of protein phosphatase PP2C$\alpha$ efficiently down-regulates PAK1 during hyper-osmotic responses. PAK1 is targeted to focal adhesions through binding to PIX and GIT (36); a significant fraction of focal adhesions contains PAK in the basal state (Fig. 5*A*). Where does PP2C$\alpha$ target and dephosphorylate the activated kinase? Although POPX (20) also binds to PIX to maintain PAK1 in the inactive state, its binding site overlaps GIT1 and therefore does not participate in regulation of PAK in the focal adhesion compartment. The process of PAK1 activation involves autophosphorylation at multiples sites including $Ser^{198/203}$ (36). This can lead to a decrease in PIX-PAK1 binding but nonetheless, that anti-$Ser(P)^{198/203}$ stains adhesions suggests a pool of activated kinase exists at this site. Under osmotic activation of the kinase it is clearly translocated away from focal adhesions *versus* GIT1 and into a perinuclear compartment (Fig. 5, *A* and *B*). Because the relative levels of GIT1/PIX and PAK are not established, there is no conclusive data that PAKs operate away from the complex. Overexpressed PP2C$\alpha$ was observed to be more concentrated at focal adhesions under osmotic stress (supplemen-

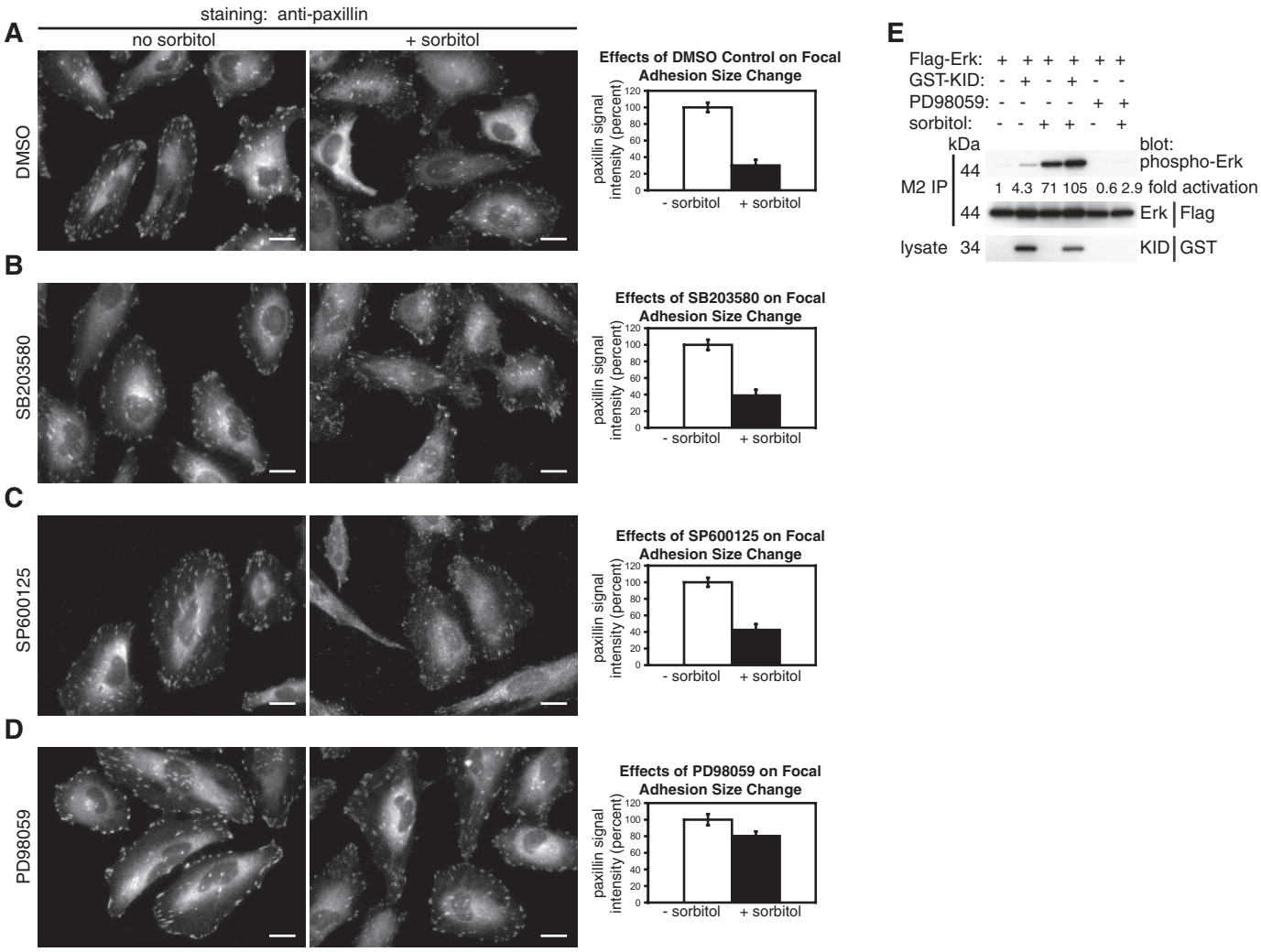


FIGURE 7. **Effects of MAPK inhibition on osmo-induced focal adhesion disassembly.** *A*, HeLa cells were treated with DMSO control (0.1% final concentration) for 1 h before sorbitol treatment. Focal adhesions of cells not sorbitol-induced were standardized to 100% (from paxillin fluorescence levels) and used to compare with focal adhesions of sorbitol-induced cells. Statistics are detailed in supplemental Table C. *B*, HeLa cells were treated with 20 μM SB203580 for 1 h before sorbitol treatment. Focal adhesion analysis was performed as in *A*. *C*, HeLa cells were treated with 30 μM SP600125 for 1 h before sorbitol treatment. Focal adhesion analysis was performed as above. *D*, HeLa cells were treated with 30 μM PD98059 for 1 h before sorbitol treatment. *Bars* on images are equivalent to 20 μm; two independent fields were analyzed for quantitation. *E*, COS7 cells were transfected with FLAG-ERK, with or without GST-KID. Cells were left untreated or induced with sorbitol, and FLAG-ERK immunoprecipitates were analyzed by Western blotting against phospho-ERK. Densitometry of blots was used for quantitation of osmo-induced ERK activation. The level of phospho-ERK in the first lane was standardized to 1 and used for comparison against other samples. For positive control of MEK-ERK inhibition in this assay, cells were treated with 30 μM PD98059 for 1 h before sorbitol treatment, in the *fifth* and *sixth lanes*.

tal Fig. S3*B*), and conceivably can block PAK activation at focal adhesions and in the cytosol. In our co-precipitation analyses, we did not detect significant PP2Cα interaction with PAK1, suggesting the phosphatase does not target PAK through direct binding or that the interaction is too transient for a biochemical assay. Endogenous PAK1 protein purified from rat or bovine brain lysate or recombinant kinase from mammalian cells is essentially inactive (26). In contrast, the recombinant protein purified from *E. coli* is activated and the presence of such active kinase in cells is toxic to bacteria when grown at 37 °C.[3] Because native rat brain extracts can robustly inhibit activation of recombinant PAK1, we infer that the same phosphatase component of mammalian cells keeps the kinase in check upon cycles of activation-inactivation. Our results suggest that although the dominant biochemical activity toward PAK in brain lysate is PP2Cα (Fig. 1), this phosphatase has specificity toward osmotic activated kinase in cell culture. As PAK activation has not been studied in primary neuronal cultures it would be of interest to examine the situation there.

*PAKs Function in Stress-induced MAPK Signaling*—Our results suggest PAK1 is closely linked to p38 in hyperosmotic signaling. First, PAK1 was most potently activated by sorbitol relative to the effects of serum, epidermal growth factor, or platelet-derived growth factor (Fig. 2*A*). Second, the time scale of PAK1 activation upon sorbitol treatment closely resembled that of p38 (Fig. 2*B*), and third, all three isoforms of PAK are recruited to the p38 MAPK complex after osmotic shock in their active state (Fig. 2*C*). This could represent a conserved process, as budding yeast PAK homolog Ste20 was recruited to the Hog MAPK complex (37). The recruitment of PAK1 was dependent on its phosphorylation (Fig. 2*E*) and unlikely to involve direct interaction, as only ~2% of HA-PAK1 was recov-

[3] P. M. Chan, L. Lim, and E. Manser, unpublished observations.

ered with overexpressed FLAG-p38 (data not shown). Candidates for PAK1 recruitment would be proteins assembled into the p38 complex, such as the scaffolding protein OSM (38).

Our results also suggest redundancy of group I PAKs in the p38 pathway. Overexpression of the group I PAK isoforms can augment p38 phosphorylation (Fig. 2*D*) and the overexpression of KID, which targets all group I PAKs, resulted in robust inhibition of the p38 response (Figs. 3*C* and 4*B*). Consistent with this, siRNA targeting PAK reduced p38 activation (Fig. 3*B*). Our siRNA design based on the amino terminus of PAK1 (bases 9–1012) is expected to act on PAK2 and PAK3 (which are at lower levels) because of significant nucleotide identity in well conserved regions.

*Phosphatase-mediated Tuning of p38 Response to Stress Signaling*—MAPK activation after osmotic stress is well recognized in cellular homeostasis (12), with fine-tuning of the MAPK complex, which provides transcriptional control of genes that balance intracellular osmotic pressure. In support of this, the levels of phosphorylated MAPKs are proportionate to the osmotic stress applied (Fig. 2*C*). Our findings correlate with a number of studies that have implicated PP2C phosphatases as negative regulators of stress-activated MAPK pathways (25, 43, 44). PP2C$\alpha$ has been shown to dephosphorylate and inactivate mitogen-activated protein kinase kinase 6 (MKK6) and SAPK/ERK kinase 1 (SEK1) as well as p38. PP2C$\beta$ associates with and down-regulates transforming growth factor $\beta$-activated kinase 1 (TAK1) and its downstream targets p38 and JNK (45). On the other hand, the MAPK dual-specificity phosphatases have also been shown to be important regulators of MAPK signaling. In HeLa cells, MKP1 has been shown to mediate anti-inflammation through inhibition of p38 (46) and in *Caenorhabditis elegans*, a MKP7 ortholog VHP1 is reported to down-regulate KGB1, an ortholog of mammalian Jnk1 and is involved in heavy metal sensitivity (47). The MAPK dual-specificity phosphatases may also have roles in regulating MAPK pathways in hyperosmotic response, perhaps after the acute phase of osmotic stress.

PP2C$\alpha$ is a monomeric enzyme with no known mechanism of regulation other than divalent cation dependence (48). However, in common with other phosphatases it is likely to be the coupling to particular protein complexes that are specific targets. In our confocal images we observed the translocation of the phosphatase to paxillin-residing areas after osmotic shock (supplemental Fig. S3*B*). PP2C$\alpha$ does not appear to affect cytoskeletal dynamics in the absence of stimulus, as the overexpressed phosphatase had no obvious effect on focal adhesions (Fig. 6*A*) or filamentous actin (data not shown) in untreated cells. In our model of osmotic stress signaling (Fig. 8), high extracellular solute concentration turns on the cellular osmosensing machinery and leads to activation of PAK and other kinases upstream of the MAPK cascade that act on p38. Experiments with PP2C$\alpha$ knockdown indicate phosphatase levels are limiting with respect to cellular responses via PAK and p38 activation in osmotic stress (Fig. 3*B*).

*Multiple Signals Govern PAK1 Activation in Hyperosmotic Signaling*—The hyperosmotic response signals to components involved in maintaining cellular integrity, and our present study identified PAK as a potential component of the osmosensing machinery. We have identified PI3K and Cdc42 activities, as

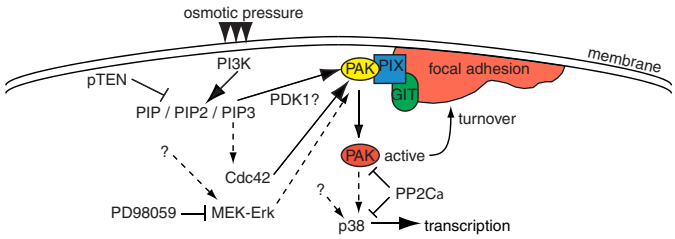


FIGURE 8. **Signaling through PAK in the hyperosmotic response pathway.** Increased osmotic pressure signals to PI3K, resulting in the accumulation of phosphoinositides, which can be reversed by pTEN activity. This may lead to recruitment and activation of downstream effectors such as PDK1 and RhoGEFs through their pleckstrin homology domains. PAK may be activated by Cdc42 via RhoGEF activity or directly by PDK1 phosphorylation. PAK binding to its partners PIX and GIT1, which targets the kinase to focal adhesions, is required for its activation. Osmotic pressure also activates MAPK signaling, and the MEK-ERK pathway is required for stress-induced focal adhesion disassembly and full PAK activation. It is unclear whether phosphoinositide generation links to MEK-ERK activation and whether MEK or ERK directly phosphorylates PAK in this pathway. Activated PAK acts locally at focal adhesions to promote turnover but also dissociates from them and targets to the p38 complex, which in turn regulates transcriptional response. A PAK-independent pathway is also likely to act on p38, as PAK inhibition by KID overexpression did not fully abolish p38 phosphorylation. PP2C$\alpha$ may act on focal adhesion-associated PAK and on the dissociated PAK and p38 complex to down-regulate the MAPK response. *Dashed lines* represent intermediate or unknown steps between the signaling components.

well as PAK1 binding to Cdc42 and PIX (Fig. 4, *B–E*), to be necessary for full activation of the kinase in this response pathway. This is consistent with studies in yeast, where Cdc42 acts upstream of the PAK homolog Ste20 to activate the p38 homolog Hog1 (37). We rule out the NCK adaptor protein because PAK binding to NCK is dispensable for full activation (Fig. 4*C*) and no NCK was detected in stress-activated PAK co-precipitates (data not shown). PI3K has been shown to be involved in the hyperosmotic response through elevation of $PI(3,4,5)P_3$ levels (39, 49, 50). Furthermore, PI3K has been reported to associate with the $NH_2$ terminus of PAK1 (40). Overexpression of the lipid phosphatase pTEN abolished PAK1 activation (Fig. 4*E*), suggesting that the phospholipid products of PI3K activity are required in this pathway. Thus, PI3K may be acting on PAK1 in various ways: 1) indirectly through recruitment of the phosphatidylinositol (3,4,5)-triphosphate-dependent kinase PDK1, which has been reported to phosphorylate and activate PAK (41); 2) directly by recruiting PAK via the p110 catalytic subunit to the plasma membrane; 3) recruitment of $\alpha$PIX to the p85 subunit via a polyproline-SH3 interaction (42) or $\beta$PIX through phosphoinositide binding to the pleckstrin homology domain of $\beta$PIX (51), therefore bringing PAK in complex with PIX to the plasma membrane. We did not observe PAK1 association with p110 in co-precipitates (data not shown) nor its translocation to the plasma membrane upon sorbitol treatment (Fig. 5*A*). It is possible that a minor fraction of PAK below detectable threshold levels is recruited to the plasma membrane and that fraction is sufficient for kinase activation through autophosphorylation amplification. We do not know whether phosphoinositide binding to PIX plays a role in the activation of PAK in the context of its native PAK-PIX-GIT multimeric complex. In this scenario, phosphoinositide binding to PIX may induce conformational changes in PAK leading to kinase activation. The PAK mutant defective in PIX-binding was not activated by sorbitol treatment (Fig. 4*C*) suggesting that the kinase was acti-

vated in the context of its native complex with other partners. PAK translocated away from focal adhesions, whereas GIT1 remained associated with them after sorbitol treatment, suggesting that the activated kinase dissociated from the PIX/GIT1-containing focal adhesion complexes (Fig. 5, *A* and *B*). This translocation appears to be associated with sorbitol-induced PAK activation, as cells overexpressing PP2Cα showed a more punctate PAK staining that may correlate with increased residual localization to focal adhesions (supplemental Fig. S3*A*). Interestingly, the MEK inhibitor PD98059 significantly blocked sorbitol-induced PAK activation (Fig. 4*D*) and protected focal adhesions from disassembly (Fig. 7*D*). ERK has been shown to regulate paxillin dynamics (52) and promote FAK-paxillin association (53). PAK signaling has been reported to be upstream of the MEK-ERK in growth factor signaling (54). Our results suggest that in osmotic stress signaling, MEK-ERK signaling is upstream of PAK, as PAK inhibition had no effect on sorbitol-induced ERK phosphorylation (Fig. 7*E*). This is consistent with a recent report that PAK1 and ERK colocalize in cells plated on fibronectin and phospho-ERK precipitates with PAK in pulldown assays (55). The study also showed MEK inhibition resulted in decreased PAK activation in response to platelet-derived growth factor. Another study showed that PAK6, a member of the group II PAKs, was efficiently phosphorylated at $Ser^{560}$ by MKK6, a dual-specificity protein kinase that is upstream of p38 (56). This phosphosite motif in PAK6 is conserved in group I and II PAKs. These two reports suggest that PAK can be targeted by MAPKK and MAPK protein kinases. The levels of protection from focal adhesion disassembly conferred by PAK inhibition through KID expression and by MEK inhibition through drug treatment are essentially the same (Figs. 6*B* and 7*D*, supplemental Tables B and C), suggesting that MEK-ERK and PAK are operating in the same pathway. Although p38 is targeted by PAK in the osmo-response, chemical inhibition of p38 had no effect on focal adhesion dynamics (Fig. 7*B*), suggesting that distinct functions are performed by different MAPKs. Considering these results together, we propose a signaling scheme for osmotic stress (Fig. 8) with the following characteristics: 1) elevation of phosphoinositides that leads to Cdc42-mediated activation of PAK in complex with PIX/GIT1; 2) activation of MAPK pathways in which MEK-ERK is required for full focal adhesion disassembly; 3) translocation of activated PAK away from focal adhesions; 4) concentration of cytosolic PP2Cα in focal adhesions; and 5) induction of transient complex formation between activated PAK and p38 for full MAPK phosphorylation, which is subjected to negative regulation by PP2Cα.

*Acknowledgments—Dr. Susanne Klumpp kindly provided the PP2Cα cDNA and Dr. Xinmin Cao provided constructs of MAPKs.*

## REFERENCES


1. Manser, E., Leung, T., Salihuddin, H., Zhao, Z. S., and Lim, L. (1994) *Nature* **367,** 40–46
2. Manser, E., and Lim, L. (1999) *Prog. Mol. Subcell. Biol.* **22,** 115–133
3. Bokoch, G. M. (2003) *Annu. Rev. Biochem.* **72,** 743–781
4. Cotteret, S., Jaffer, Z. M., Beeser, A., and Chernoff, J. (2003) *Mol. Cell. Biol.* **23,** 5526–5539
5. Schurmann, A., Mooney, A. F., Sanders, L. C., Sells, M. A., Wang, H. G., Reed, J. C., and Bokoch, G. M. (2000) *Mol. Cell. Biol.* **20,** 453–461
6. Chaudhary, A., King, W. G., Mattaliano, M. D., Frost, J. A., Diaz, B., Morrison, D. K., Cobb, M. H., Marshall, M. S., and Brugge, J. S. (2000) *Curr. Biol.* **10,** 551–554
7. King, A. J., Sun, H., Diaz, B., Barnard, D., Miao, W., Bagrodia, S., and Marshall, M. S. (1998) *Nature* **396,** 180–183
8. Wang, R. A., Mazumdar, A., Vadlamudi, R. K., and Kumar, R. (2002) *EMBO J.* **21,** 5437–5447
9. Bagrodia, S., Derijard, B., Davis, R. J., and Cerione, R. A. (1995) *J. Biol. Chem.* **270,** 27995–27998
10. Frost, J. A., Steen, H., Shapiro, P., Lewis, T., Ahn, N., Shaw, P. E., and Cobb, M. H. (1997) *EMBO J.* **16,** 6426–6438
11. Burg, M. B., Kwon, E. D., and Kultz, D. (1997) *Annu. Rev. Physiol.* **59,** 437–455
12. de Nadal, E., Alepuz, P. M., and Posas, F. (2002) *EMBO Rep.* **3,** 735–740
13. Rosette, C., and Karin, M. (1996) *Science* **274,** 1194–1197
14. Chan, W. H., Yu, J. S., and Yang, S. D. (1999) *J. Cell Physiol.* **178,** 397–408
15. Roig, J., Huang, Z., Lytle, C., and Traugh, J. A. (2000) *J. Biol. Chem.* **275,** 16933–16940
16. Zhao, Z. S., Manser, E., Chen, X. Q., Chong, C., Leung, T., and Lim, L. (1998) *Mol. Cell. Biol.* **18,** 2153–2163
17. Lei, M., Lu, W., Meng, W., Parrini, M. C., Eck, M. J., Mayer, B. J., and Harrison, S. C. (2000) *Cell* **102,** 387–397
18. Chong, C., Tan, L., Lim, L., and Manser, E. (2001) *J. Biol. Chem.* **276,** 17347–17353
19. Loo, T. H., Ng, Y. W., Lim, L., and Manser, E. (2004) *Mol. Cell. Biol.* **24,** 3849–3859
20. Koh, C. G., Tan, E. J., Manser, E., and Lim, L. (2002) *Curr. Biol.* **12,** 317–321
21. Westphal, R. S., Coffee, R. L., Jr., Marotta, A., Pelech, S. L., and Wadzinski, B. E. (1999) *J. Biol. Chem.* **274,** 687–692
22. Zhan, Q., Ge, Q., Ohira, T., Van Dyke, T., and Badwey, J. A. (2003) *J. Immunol.* **171,** 3785–3793
23. Xia, C., Ma, W., Stafford, L. J., Marcus, S., Xiong, W. C., and Liu, M. (2001) *Proc. Natl. Acad. Sci. U. S. A.* **98,** 6174–6179
24. Kissil, J. L., Wilker, E. W., Johnson, K. C., Eckman, M. S., Yaffe, M. B., and Jacks, T. (2003) *Mol. Cell* **12,** 841–849
25. Takekawa, M., Maeda, T., and Saito, H. (1998) *EMBO J.* **17,** 4744–4752
26. Manser, E., Huang, H. Y., Loo, T. H., Chen, X. Q., Dong, J. M., Leung, T., and Lim, L. (1997) *Mol. Cell. Biol.* **17,** 1129–1143
27. Chan, P. M., Ilangumaran, S., La Rose, J., Chakrabartty, A., and Rottapel, R. (2003) *Mol. Cell. Biol.* **23,** 3067–3078
28. Manser, E., Chong, C., Zhao, Z. S., Leung, T., Michael, G., Hall, C., and Lim, L. (1995) *J. Biol. Chem.* **270,** 25070–25078
29. Cohen, P. (1989) *Annu. Rev. Biochem.* **58,** 453–508
30. Miah, S. M., Sada, K., Tuazon, P. T., Ling, J., Maeno, K., Kyo, S., Qu, X., Tohyama, Y., Traugh, J. A., and Yamamura, H. (2004) *Mol. Cell. Biol.* **24,** 71–83
31. Clerk, A., and Sugden, P. H. (1997) *FEBS Lett.* **403,** 23–25
32. Hanada, M., Kobayashi, T., Ohnishi, M., Ikeda, S., Wang, H., Katsura, K., Yanagawa, Y., Hiraga, A., Kanamaru, R., and Tamura, S. (1998) *FEBS Lett.* **437,** 172–176
33. Vadlamudi, R. K., and Kumar, R. (2003) *Cancer Metastasis Rev.* **22,** 385–393
34. Bokoch, G. M., Reilly, A. M., Daniels, R. H., King, C. C., Olivera, A., Spiegel, S., and Knaus, U. G. (1998) *J. Biol. Chem.* **273,** 8137–8144
35. King, C. C., Gardiner, E. M., Zenke, F. T., Bohl, B. P., Newton, A. C., Hemmings, B. A., and Bokoch, G. M. (2000) *J. Biol. Chem.* **275,** 41201–41209
36. Zhao, Z. S., Manser, E., and Lim, L. (2000) *Mol. Cell. Biol.* **20,** 3906–3917
37. Raitt, D. C., Posas, F., and Saito, H. (2000) *EMBO J.* **19,** 4623–4631
38. Uhlik, M. T., Abell, A. N., Johnson, N. L., Sun, W., Cuevas, B. D., Lobel-Rice, K. E., Horne, E. A., Dell'Acqua, M. L., and Johnson, G. L. (2003) *Nat. Cell Biol.* **5,** 1104–1110
39. Meier, R., Thelen, M., and Hemmings, B. A. (1998) *EMBO J.* **17,**

7294–7303
40. Papakonstanti, E. A., and Stournaras, C. (2002) *Mol. Biol. Cell* **13,** 2946–2962
41. Cohen, P., Alessi, D. R., and Cross, D. A. (1997) *FEBS Lett.* **410,** 3–10
42. Yoshii, S., Tanaka, M., Otsuki, Y., Wang, D. Y., Guo, R. J., Zhu, Y., Takeda, R., Hanai, H., Kaneko, E., and Sugimura, H. (1999) *Oncogene* **18,** 5680–5690
43. Meskiene, I., Bogre, L., Glaser, W., Balog, J., Brandstotter, M., Zwerger, K., Ammerer, G., and Hirt, H. (1998) *Proc. Natl. Acad. Sci. U. S. A.* **95,** 1938–1943
44. Warmka, J., Hanneman, J., Lee, J., Amin, D., and Ota, I. (2001) *Mol. Cell. Biol.* **21,** 51–60
45. Hanada, M., Ninomiya-Tsuji, J., Komaki, K., Ohnishi, M., Katsura, K., Kanamaru, R., Matsumoto, K., and Tamura, S. (2001) *J. Biol. Chem.* **276,** 5753–5759
46. Lasa, M., Abraham, S. M., Boucheron, C., Saklatvala, J., and Clark, A. R. (2002) *Mol. Cell. Biol.* **22,** 7802–7811
47. Mizuno, T., Hisamoto, N., Terada, T., Kondo, T., Adachi, M., Nishida, E., Kim, D. H., Ausubel, F. M., and Matsumoto, K. (2004) *EMBO J.* **23,** 2226–2234
48. Price, N. E., and Mumby, M. C. (1999) *Curr. Opin. Neurobiol.* **9,** 336–342
49. Manser, E., Loo, T. H., Koh, C. G., Zhao, Z. S., Chen, X. Q., Tan, L., Tan, I., Leung, T., and Lim, L. (1998) *Mol. Cell* **1,** 183–192
50. Zhang, Z., Yang, X. Y., Soltoff, S. P., and Cohen, D. M. (2000) *Am. J. Physiol.* **278,** F155–F164
51. Park, H. S., Lee, S. H., Park, D., Lee, J. S., Ryu, S. H., Lee, W. J., Rhee, S. G., and Bae, Y. S. (2004) *Mol. Cell. Biol.* **24,** 4384–4394
52. Pollock, C. B., Shirasawa, S., Sasazuki, T., Kolch, W., and Dhillon, A. S. (2005) *Cancer Res.* **65,** 1244–1250
53. Liu, Z. X., Yu, C. F., Nickel, C., Thomas, S., and Cantley, L. G. (2002) *J. Biol. Chem.* **277,** 10452–10458
54. Eblen, S. T., Slack, J. K., Weber, M. J., and Catling, A. D. (2002) *Mol. Cell. Biol.* **22,** 6023–6033
55. Sundberg-Smith, L. J., Doherty, J. T., Mack, C. P., and Taylor, J. M. (2005) *J. Biol. Chem.* **280,** 2055–2064
56. Kaur, R., Liu, X., Gjoerup, O., Zhang, A., Yuan, X., Balk, S. P., Schneider, M. C., and Lu, M. L. (2005) *J. Biol. Chem.* **280,** 3323–3330
57. Bain, J., Plater, L., Elliott, M., Shpiro, N., Hastie, C. J., McLauchlan, H., Klevernic, I., Arthur, J. S. C., Alessi, D. R., and Cohen, P. (2007) *Biochem. J.* **408,** 297–315